nature chemistry

Article

https://doi.org/10.1038/s41557-022-01106-9

Active template strategy for the preparation of π-conjugated interlocked nanocarbons

Received: 29 March 2022

Accepted: 3 November 2022

Published online: 12 January 2023

Check for updates

James H. May[1], Jeff M. Van Raden[1], Ruth L. Maust[1], Lev N. Zakharov[2] & Ramesh Jasti[1]

Mechanically interlocked carbon nanostructures represent a relatively unexplored frontier in carbon nanoscience due to the dificulty in preparing these unusual topological materials. Here we illustrate an active-template method in which a [*n*]cycloparaphenylene precursor macrocycle is decorated with two convergent pyridine donors that coordinate to a metal ion. The metal ion catalyses alkyne–alkyne cross-coupling reactions within the central cavity of the macrocycle, and the resultant interlocked products can be converted into fully π-conjugated structures in subsequent synthetic steps. Specifically, we report the synthesis of a family of catenanes that comprise two or three mutually interpenetrating [*n*]cycloparaphenylene-derived macrocycles of various sizes. Additionally, a fully π-conjugated [3]rotaxane was synthesized by the same method. The development of synthetic methods to access mechanically interlocked carbon nanostructures of varying topology can help elucidate the implications of mechanical bonding for this emerging class of nanomaterials and allow structure–property relationships to be established.

The optical and electronic properties of carbon nanostructures are linked to their precise three-dimensional arrangement of carbon atoms. Graphene, fullerene and carbon nanotubes, although they share very similar local bonding environments (that is, exclusively sp^2-hybridized bonded carbon), display vastly different physical properties due to the differing topologies of the overall structure[1]. In recent years, bottom-up organic synthesis strategies have enabled carbon nanostructures to be prepared that were inaccessible by more traditional thermodynamically driven methods. For example, substructures of carbon nanotubes, often referred to as carbon nanohoops[2] and carbon nanobelts[3–5], can now be prepared in which the size[6], connectivity[7] and even heteroatom doping[8] can be controlled with atomic precision. These molecular nanocarbons are gaining traction for a wide array of possible applications in organic electronics, biology and polymer science[9–13]. A particularly exciting avenue is to use organic synthetic methods to prepare topologically unique carbon nanomaterials—in particular, mechanically interlocked structures. In 2019, Itami co-workers used a traceless silyl tethering strategy for the syntheses of catenanes and a trefoil knot composed entirely of *para*-linked phenylene units (Fig. 1a)[14]. The catenated and knotted molecules are structurally related to the [*n*]cycloparaphenylenes ([*n*]CPPs), but the unique topologies of these structures give rise to dynamic motion and optical characteristics that differ from those of the parent [*n*]CPPs. General synthetic methods to access a wide array of interlocked carbon nanostructures in which the structures can be altered via connectivity, size and heteroatom doping would bring about a class of dynamic nanomaterials with engineerable optical and electronic properties. Here we disclose a versatile active-template (AT) methodology that can deliver an array of mechanically interlocked nanocarbons of the catenane and rotaxane type, composed entirely of π-conjugated units (Fig. 1b).

Results and discussion

Method design

In 2006, Leigh and co-workers introduced the AT approach to mechanically interlocked molecules[15]. In contrast to the more common passive-template approaches[16,17], the templating moiety in this

[1]Department of Chemistry and Biochemistry, Materials Science Institute, and Knight Campus for Accelerating Scientific Impact, University of Oregon, Oregon, USA. [2]CAMCOR—Center for Advanced Materials Characterization in Oregon, University of Oregon, Oregon, USA. e-mail: rjasti@uoregon.edu

https://doi.org/10.1038/s41557-022-01106-9

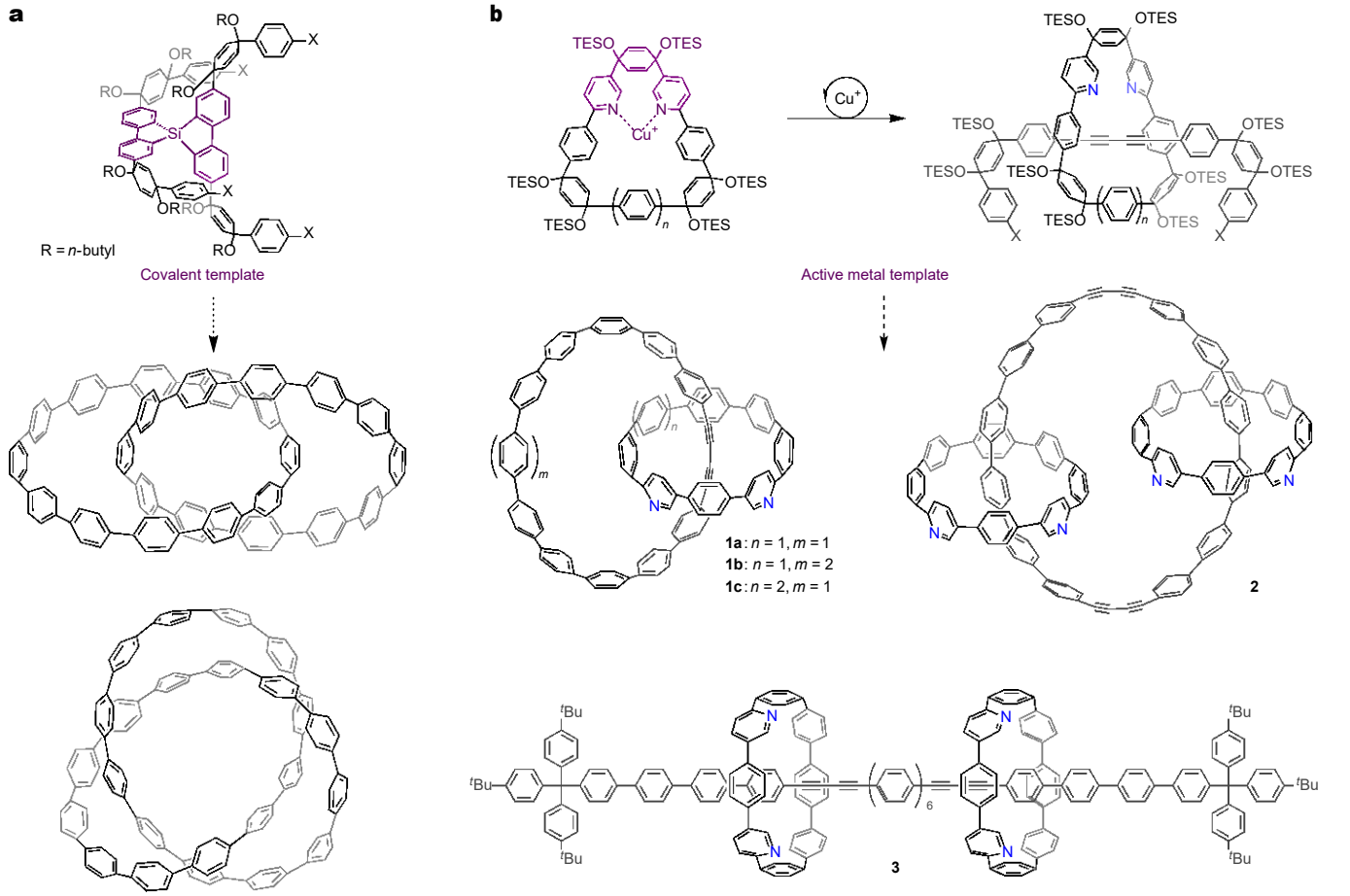

Fig. 1 | Methods to synthesize π-conjugated interlocked nanocarbon species. a, Itami and co-workers' covalent silicon tethering approach to all benzene catenanes and trefoil knots[14]. **b**, AT strategy for the synthesis of π-conjugated [*n*]catenanes **1a**–**1c**, **2** (*n* = 2 or 3) and π-conjugated [3]rotaxane **3**.

case is actively involved in the formation of the mechanical bond. Specifically, the AT approach relies on a macrocycle to coordinate a catalytic metal ion endotopically (that is, at the interior of its cavity). Bond-forming reactions are then facilitated by this metal, which results in a product molecule that is threaded through the centre of the macrocycle. Provided the threaded species is appropriately functionalized with large 'stopper' groups at either end, the 'thread' unit becomes mechanically entrapped and unable to diffuse away from the macrocycle. AT offers certain advantages over the passive template in that the breadth of structures that may be formed are not dictated by the inherent molecular recognition between interlocking components, but by the catalytic character of the templating metal ion. Indeed, since the initial report by Leigh, Denis and Goldup among others showed the remarkable structural diversity and range of applications enabled by this strategy[18]. Macrocycles with radial π systems, such as [*n*]CPPs, however, are challenging motifs to use in AT approaches due to their lack of inwardly directed functional groups that might facilitate the required endotopic metal coordination[19–22]. We envisioned an approach in which macrocyclic [*n*]CPP precursors, rather than the final aromatized structures, are used for the AT reaction. The methods developed in our lab to synthesize [*n*]CPPs centre on the use of cyclohexadiene motifs as bent units that allow for the construction of low-strain macrocyclic precursors, which are ultimately converted into π-conjugated molecules via reductive aromatization[2]. Advantageously, these precursors were prepared with a wide-ranging structural diversity, which includes non-benzenoid aromatics, heterocycles and even antiaromatic molecules[8]. We envisioned that these same cyclohexadiene systems might also provide the basis for a ligand motif that could enable CPP precursors to endotopically coordinate metal ions. We hypothesized that macrocyclic structures that contain a cyclohexadiene motif with two flanking pyridine rings would provide a general active templating system to prepare a wide array of π-conjugated, interlocked structures.

To assess the viability of this approach, pyridine-containing macrocycles **4a** and **4b** (Fig. 2) were prepared in high yields and on the gram and half-gram scale, respectively (Supplementary Information). Half-axle thread components were designed to be analogous to commonly used synthons in CPP syntheses but carrying a terminal alkyne (**5a**) or alkyne bromide (**5b**) functional group handle for the AT reaction. The Cu^{I}-catalysed active-template Cadiot–Chodkiewicz (AT-CC) reaction was chosen for this study as it is well established in mechanically interlocked molecule syntheses and allows for the creation of fully π-conjugated thread molecules[23,24]. Moreover, if so desired, the resultant diyne is easily converted into other π-conjugated units. We anticipated that the triethylsilyl (TES) ether substituents of **5a** and **5b** would provide a sufficient steric bulk to serve as stopper units to prevent dethreading of the internally cross-coupled species. Accordingly, we envisioned accessing [2]rotaxane molecules that may serve as precursors to catenated structures consisting of a diaza[*n*]CPP and an [*n* + 2]CPP, where the +2 of the latter denotes the *sp*-carbon atoms of the 1,4-butadyine moiety embedded in the CPP backbone.

[*n*]catenane synthesis

Gratifyingly, both macrocycles **4a** and **4b** efficiently template the AT-CC reaction to afford [2]rotaxanes **6a** and **6b** in a 65 and 53% yield,

https://doi.org/10.1038/s41557-022-01106-9

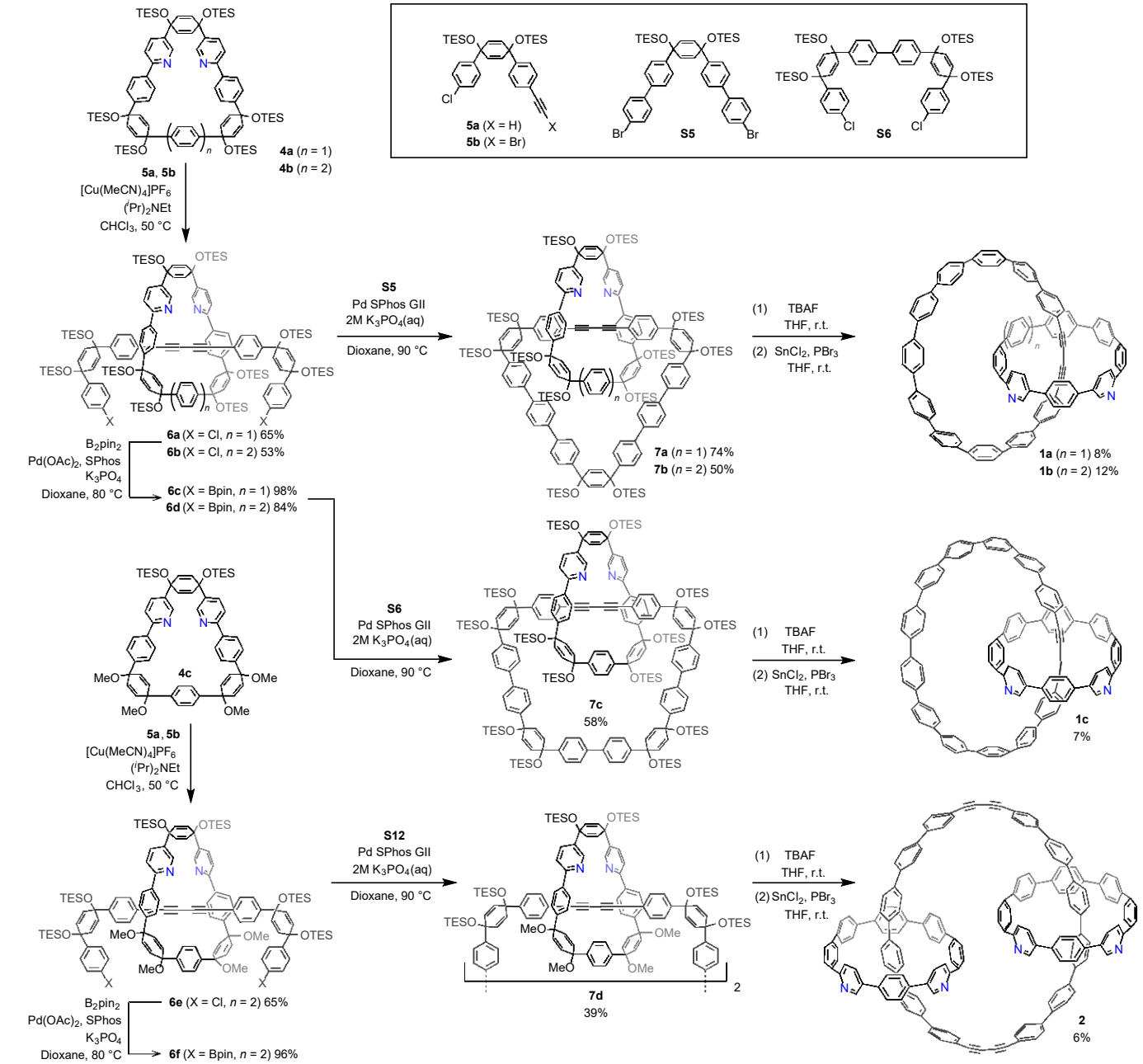

Fig. 2 | Preparation of π-conjugated catenanes. Synthetic routes to compounds **1a**–**1c** and **2**. The general synthetic path to the final π-conjugated catenanes is as follows: AT-CC threading of macrocyclic ligands **4a**–**4c** to give [2]rotaxane intermediates **6a**, **6b** and **6e**; Miyuara borylation reactions to give [2]rotaxanes **6c**, **6d** and **6f** with pinacol boronic ester (Bpin)-terminated thread components; Suzuki–Miyuara cross coupling macrocyclization of [2]rotaxanes to give [2]catenanes **7a**–**7c** or [3]catenane **7d**; reductive aromatization of the cyclohexadiene moieties in **7a**–**7d** to furnish fully π-conjugated [2]catenanes **1a**–**1c** and [3]catenane **2**. B_2pin_2, bis(pinacolato)diboron; $(^iPr)_2NEt$, *N*,*N*-diisopropylethylamine; Pd SPhos GII, chloro(2-dicyclohexylphosphino-2′, 6′-dimethoxy-1,1′-biphenyl)[2-(2′-amino-1,1′-biphenyl)]palladium(II); r.t., room temperature; SPhos, dicyclohexylphosphino-2′,6′-dimethoxybiphenyl; TBAF, tetra-*n*-butylammonium fluoride.

respectively, provided excess (2.5 equiv.) of the coupling partners (**5a** and **5b**) are used (Fig. 2). [2]Rotaxanes **6a** and **6b** are subsequently transformed into the corresponding bis-boronates, **6c** and **6d**, via a Miyaura borylation reaction. Under dilute Suzuki–Miyaura cross-coupling conditions, **6c** and **6d** react with **S5** to afford [2]catenanes **7a** and **7b** in a 74 and 50% yield, respectively. Subjecting **6c** to similar macrocyclization reaction conditions using the alternative coupling partner **S6** afforded [2]catenane **7c** in a 58% yield. This demonstrates the modularity of these methods whereby [2]catenanes may be accessed, in which the size of both the templating macrocycle and the secondary macrocycle formed in the last step may be varied. Aromatization reactions were performed via conditions adapted from those developed by Yamago and co-workers[25] to provide **1a**, **1b** and **1c** in a 7, 11 and 6% yield, respectively. Although the yields for these final transformations are low, weighable quantities of the final compounds, sufficient for their characterization, could be obtained (a more detailed discussion of the issues associated with the reductive aromatization reactions is provided on Supplementary page 111). In an attempt to access higher-order interlocked molecules, **6a** and **6c** were subjected to dilute Suzuki–Miyaura cross-coupling to target a [3]catenane. This reaction,

https://doi.org/10.1038/s41557-022-01106-9

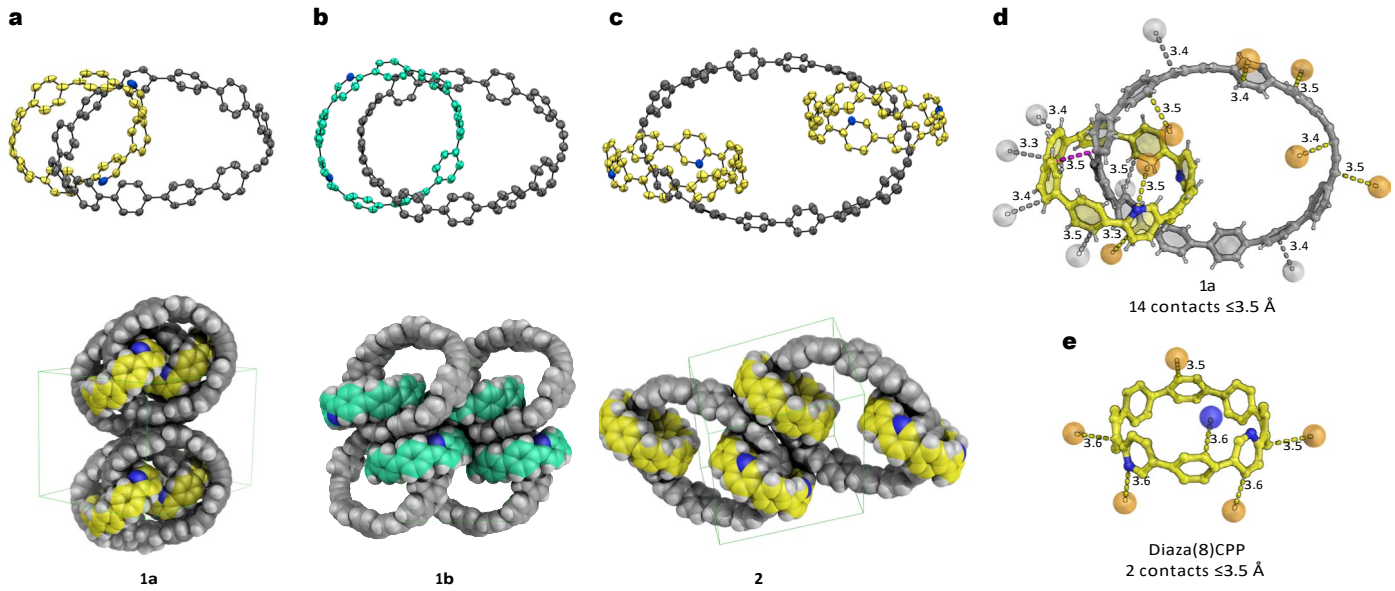

Fig. 3 | X-ray structures of 1a, 1b and 2. a–**c**, Structures of **1a** (**a**), **1b** (**b**) and **2** (**c**). Top: ORTEP (Oakridge thermal ellipsoid) drawings with thermal ellipsoids set to a 50% probability with the hydrogen atoms and solvent molecules omitted for clarity. Bottom: packing of the structures. Carbon, grey, yellow or green to distinguish different macrocycles; nitrogen, blue; hydrogen, white; solvent molecules omitted for clarity. **d**,**e**, Short contacts (Å) observed in the X-ray structures of **1a** (**d**) and diaza[8]CPP (**e**) demonstrating the relatively large number of close contacts (distance ≲3.5 Å) in the catenated versus non-catenated structures. Contacted atoms are shown as semitransparent spheres and are coloured to distinguish between those that belong to neighbouring diaza[8]CPPs (orange) and neighbouring [11 + 2]CPPs (grey). The contact drawn in magenta (**e**) shows the closest contact existing between carbon atoms of the two catenated rings. Spheres coloured blue (**e**) denote closely contacted nitrogen atoms of an adjacent diaza[8]CPP.

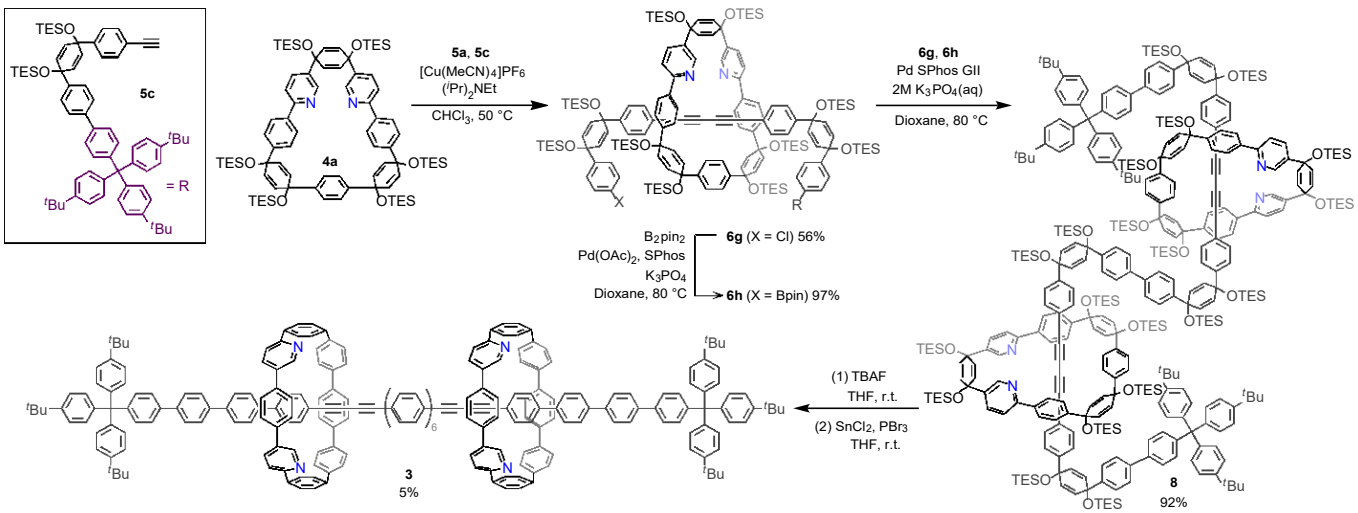

Fig. 4 | Synthesis of a fully π-conjugated [3]rotaxane. Synthetic route to compound **3**: AT-CC threading of macrocyclic ligand **4a** to give asymmetrical [2]rotaxane intermediate **6g**; Miyuara borylation reaction to give [2]rotaxane **6h** with Bpin-terminated thread components; Suzuki–Miyuara cross-coupling reaction of [2]rotaxanes **6g** and **6h** to give [3]rotaxane **8** or [3]catenane **7d**; reductive aromatization of the cyclohexadiene moieties in **8** to furnish fully π-conjugated [3]rotaxane **3**.

however, resulted only in a complex mixture of oligomeric products. Analysis of a space-filling representation (Supplementary Fig. 64) of the target molecule revealed a large degree of steric congestion created by clashing TES groups of the two pre-existing macrocycles, which probably precludes macrocyclization and favours oligomer formation. To circumvent these issues, analogous [2]rotaxane synthons, **6e** and **6f**, were prepared using the templating macrocycle **4c** in which the TES substituents on the lower half (as drawn in Fig. 2) of the macrocycle are replaced with smaller methyl ether groups. Satisfyingly, subjecting **6e** and **6f** to macrocyclization reaction conditions afforded [3]catenane **7d** in a modest yield (39%). Conversion to the aromatized structure was accomplished via conditions analogous to those used for **1a**–**1c** to afford **2** in a 6% yield. The resulting structure consists of a [12 + 4]CPP ('+4' now that there are two butadiyne moieties present) that threads two diaza[8]CPPs, a [3]catenane made up of entirely π-conjugated components.

X-ray crystallographic analysis

Single crystals suitable for X-ray analysis were grown for **1a** (Fig. 3a), **1b** (Fig. 3b) and **2** (Fig. 3c), which unambiguously confirmed their

https://doi.org/10.1038/s41557-022-01106-9

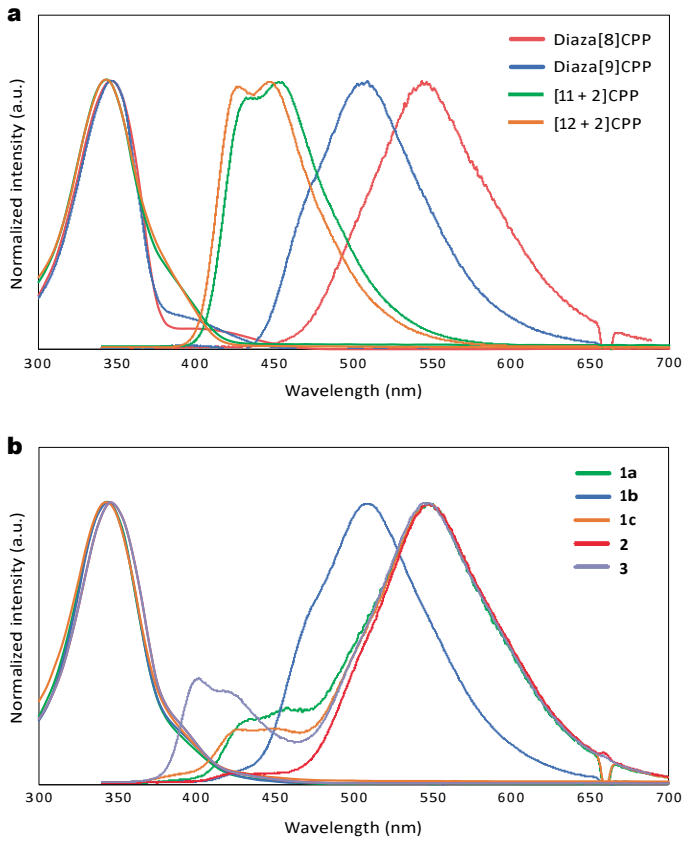

Fig. 5 | Photophysical characteristics of compounds. a, UV–vis absorbance (solid lines) and fluorescence (dashed lines) spectra of diaza[*n*]CPPs (*n* = 8 and 9) and [*n* + 2]CPPs (*n* = 11 and 12) free of mechanical linkage. **b**, UV–vis absorbance (solid lines) and fluorescence (dashed lines) spectra of interlocked structures **1a**–**1c**, **2** and **3** demonstrating the dominant emission of the diaza[*n*]CPP component(s) over the diyne-containing components. a.u., arbitrary units.

catenated structures. In the solid state, **1a** exists as a dimer in which the diaza[8]CPP of one catenane occupies the void space of the [11 + 2] CPP from its dimeric partner. Increasing the size of the diaza[*n*]CPP by one phenylene unit prevents this dimer formation, as evidenced by the solid-state structure of **1b**, which displays a much more open packing motif. In contrast to the structures of **1a** and **1b**, the diaza[8]CPPs of **2** reside over the two opposing butadiyne moieties of the mutually encapsulated [12 + 4]CPP. This shift in preference is probably do to the sterically congested nature of the structure in which the most efficient separation of mass is achieved with the two diaza[8]CPPs that exist along the major axis of the [12 + 4]CPP's elliptical structure. Indeed, the structure of the diyne-containing ring contorts substantially to accommodate the two interlocking rings, and displays impressively acute –(C–C≡C)– angles as low as 163.8° (164.8 and 164.1° for **1a** and **1b** respectively). The solid-state packing of organic molecules is directly correlated to useful materials properties, such as charge-transport characteristics[26], as well as their utility as porous molecular materials[27]. The introduction of mechanical linkages represents a unique approach to influence the crystal packing of CPPs beyond merely adjusting the diameter or atomic composition. Interestingly, many close contacts (≤3.5 Å) were observed in the crystal structures of **1a**–**1c** and **2** when compared with those in the crystal structures of diaza[8]CPP and diaza[9]CPP. Not only do the catenated structures show a greater number of these contacts, but the mean distance between contacting atoms is markedly lower. This is most dramatic in the case of **1a** (Fig. 3d) in which 14 distinct intermolecular short contacts (≤3.5 Å) are observed between non-bonded carbon (or nitrogen) atoms of a catenane and its neighbours. This is in stark contrast to the structure of diaza[8]CPP in which only two contacts exist that are ≤3.5 Å (Fig. 3e), which illustrates the large influence that catenation may have on the materials properties of molecular nanocarbons.

[3]rotaxane synthesis

Encouraged by our success in synthesizing catenated molecules, we envisioned that [2]rotaxane precursors similar to **6a**–**6f** might also be used as intermediates in the synthesis of higher-order [*n*]rotaxanes (*n* > 2) that feature fully conjugated threads. To investigate, [2]rotaxanes, **6g** and **6h**, were prepared (Fig. 4) in which ^{t}Bu-substituted trityl groups were installed on one end of the thread. This bulky substituent served as a permanent stopper that remains at the thread termini following the removal of silyl groups. [3]Rotaxane **8** was readily prepared by the Suzuki cross-coupling of **6g** and **6h** in 92% yield, which on reductive aromatization provided [3]rotaxane **3** in 5% yield. Remarkably, despite the 14 unsubstituted phenyl rings and two interspacing butadiene moieties that make up the thread, **3** was completely soluble in common organic solvents and could be characterized by ^{1}H and ^{13}C NMR spectroscopy. Given the high solubility of **3**, one might imagine that [2]rotaxanes analogous to **6a** and **6g** could serve as monomer and end-capping units, respectively, in the formation of insulated π-conjugated wires, to offer a new route to this class of electronic material. As it stands, the yields for the final reductive aromatization reaction are prohibitively low for such a pursuit; however, future work will seek alternative reaction conditions that provide a more efficient conversion to the aromatized structures.

Photophysical analysis of the interlocked structures

To examine the impact of the mechanical bond on the photophysical properties of these molecules, we independently synthesized and characterized control molecules diaza[8]CPP and diaza[9]CPP, along with [11 + 2]CPP and [12 + 2]CPP. As shown in Fig. 5, the photophysical properties of these molecules are consistent with those of the parent CPPs, with the ultraviolet–visible (UV–vis) maximum absorption independent of size ($\lambda_{max} \approx 345$ nm), but the emission maximum redshifts with decreasing size (for example, diaza[8]CPP is redshifted versus diaza[9]CPP)[28]. The photophysical characteristics of **1a–1c**, **2** and **3** were also assessed by UV–vis and fluorescence spectroscopy (Fig. 5). The UV–vis absorbance profiles of all the interlocked structures were nearly identical to those of the control molecules, each with $\lambda_{max} \approx 345$ nm. In contrast, the emission profiles of the interlocked structures varied depending on the exact composition. In each case, the dominant emission was that of the smaller diaza[*n*]CPP—**1c** had an emission maximum centred around 509 nm and **1a**, **1b**, **2** and **3** had an emission maximum centred around 550 nm. In addition to the emission from the diaza[*n*]CPP, the fluorescence profiles of each interlocked structure also displayed a weak blue shoulder that stemmed from the emission of the diyne-containing CPPs (or linear thread component in the case of **3**). As the brightness of the CPP emission is known to increase with increasing ring size[28], the rather modest contribution of the diyne-containing CPP to the catenanes' overall fluorescence profile is consistent with energy transfer from the larger hoop to the smaller hoop[14]. Further study of the photophysics of these dynamic catenane and rotaxane systems is an exciting prospect for the future.

Effect of nitrogen-atom placement on ligand behaviour

Very few types of macrocycles have been used in AT chemistry[18], typically being flexible ethereal macrocycles with embedded phenanthrene or bipyridine motifs. Owing to the unusual nature of macrocyclic ligands **4a** and **4b**, we sought to gain a better understanding of the interaction of these molecules with a Cu catalyst. Specifically, we were curious as to whether both pyridine rings are required to direct reactivity towards the interior of the macrocycle as we had originally designed. To test this, macrocycle **S15** was synthesized, which is identical to **4a** but features

https://doi.org/10.1038/s41557-022-01106-9

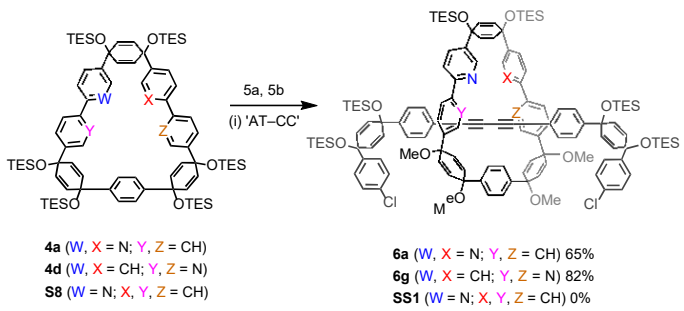

Fig. 6 | Effect of N-atom positioning on the AT reaction. [2]rotaxane yields from AT-CC reactions run using macrocyclic ligands in which the number and positioning of the N atoms were varied, highlighting the necessity for more than one N donor atom but a tolerance for their relative positions.

only a single pyridine ring. However, no interlocked products were observed for the AT-CC reactions with **S15**, which is consistent with both pyridines acting cooperatively in the endotopic binding of the Cu ion (Fig. 6). We were also interested whether alternative ligand geometries could be amenable to AT chemistry. To probe this, macrocycle **4d** was synthesized, which, like **4a**, carries two nitrogen atoms but placed at different positions along the macrocycle. Surprisingly, despite a wider bite angle and an increased distance between the two N-atom donors **4d** outperformed **4a** in the AT-CC reaction, to provide [2]rotaxane **6i** in an 82% yield (Fig. 6). Although it seems that both pyridine rings are essential in sequestering the Cu ion within the interior cavity of the macrocycle, the success of the AT-CC reaction using **4d** suggests that a bidentate binding model is probably an oversimplification of a more complex and/or dynamic interaction(s). This is significant as it demonstrates that macrocycles with atypical ligand motifs may be effectively employed in AT chemistry. As such, we anticipate that a wider array of macrocyclic motifs might be made suitable for AT chemistry than previously appreciated. Further mechanistic investigations are warranted to fully understand the nature of these unusual ligands.

Conclusion

In summary, we report a new AT synthesis by which mechanically interlocked CPPs of varying substructure and topology may be prepared. The methods disclosed in this report dramatically increase the structural space that may be explored in the context of topological nanocarbon species and lay the synthetic groundwork for the preparation of structures of even greater complexity than those presented here. Importantly, the synthetic method leverages the well-established building block approach to nanohoop architectures, which is already being employed by numerous research groups. Although we have confirmed the validity of this approach for the precursors of diaza[8]CPP and diaza[9]CPP, we anticipate that both smaller and larger macrocycles that bear these ligand motifs are capable of participating in the AT-CC reaction, which allows for a detailed analysis of the influence of the relative ring size on the properties of nanohoop catenanes. Further, owing to the simplicity of the mechanical bond-forming reaction, we envision that this AT methodology may be adapted to produce a wide array of interlocked structures, which include those decorated with functional groups or even extended polymeric materials. We anticipate that the generality of this approach will provide access to topological carbon nanostructures with emergent optical and electronic characteristics that were previously inaccessible.

Online content

Any methods, additional references, Nature Portfolio reporting summaries, source data, extended data, supplementary information, acknowledgements, peer review information; details of author contributions and competing interests; and statements of data and code availability are available at https://doi.org/10.1038/s41557-022-01106-9.

References

1. Thomas, S., Sarathchandran, C., Ilangovan, S. A. and Moreno-Pirajan, J. C. *Handbook of Carbon-Based Nanomaterials* (Elsevier, 2021).
2. Jasti, R., Bhattacharjee, J., Neaton, J. B. & Bertozzi, C. R. Synthesis, characterization, and theory of [9]-, [12]-, and [18] cycloparaphenylene: carbon nanohoop structures. *J. Am. Chem. Soc.* **130**, 17646–17647 (2008).
3. Povie, G., Segawa, Y., Nishihara, T., Miyauchi, Y. & Itami, K. Synthesis of a carbon nanobelt. *Science* **356**, 172–175 (2017).
4. Cheung, K. Y. et al. Synthesis of armchair and chiral carbon nanobelts. *Chem* **5**, 838–847 (2019).
5. Cheung, K. Y., Watanabe, K., Segawa, Y. & Itami, K. Synthesis of a zigzag carbon nanobelt. *Nat. Chem.* **13**, 255–259 (2021).
6. Darzi, E. R., Sisto, T. J. & Jasti, R. Selective syntheses of [7]–[12] cycloparaphenylenes using orthogonal Suzuki–Miyaura cross-coupling reactions. *J. Org. Chem.* **77**, 6624–6628 (2012).
7. Lovell, T. C., Colwell, C. E., Zakharov, L. N. & Jasti, R. Symmetry breaking and the turn-on fluorescence of small, highly strained carbon nanohoops. *Chem. Sci.* **10**, 3786–3790 (2019).
8. Hermann, M., Wassy, D. & Esser, B. Conjugated nanohoops incorporating donor, acceptor, hetero- or polycyclic aromatics. *Angew. Chem. Int. Ed.* **60**, 15743–15766 (2021).
9. Leonhardt, E. J. & Jasti, R. Emerging applications of carbon nanohoops. *Nat. Rev. Chem.* **3**, 672–686 (2019).
10. White, B. M. et al. Expanding the chemical space of biocompatible fluorophores: nanohoops in cells. *ACS Cent. Sci.* **4**, 1173–1178 (2018).
11. Lovell, T. C. et al. Subcellular targeted nanohoop for one- and two-photon live cell imaging. *ACS Nano* **15**, 15285–15293 (2021).
12. Peters, G. M. et al. Linear and radial conjugation in extended π-electron systems. *J. Am. Chem. Soc.* **142**, 2293–2300 (2020).
13. Huang, Q. et al. A long π-conjugated poly(*para*-phenylene)-based polymeric segment of single-walled carbon nanotubes. *J. Am. Chem. Soc.* **141**, 18938–18943 (2019).
14. Segawa, Y. et al. Topological molecular nanocarbons: all-benzene catenane and trefoil knot. *Science* **365**, 272–276 (2019).
15. Aucagne, V., Hänni, K. D., Leigh, D. A., Lusby, P. J. & Walker, D. B. Catalytic 'click' rotaxanes: a substoichiometric metal-template pathway to mechanically interlocked architectures. *J. Am. Chem. Soc.* **128**, 2186–2187 (2006).
16. Dietrich-Buchecker, C. O., Sauvage, J. P. & Kintzinger, J. P. Une nouvelle famille de molecules: les metallo-catenanes. *Tetrahedron Lett.* **24**, 5095–5098 (1983).
17. Barin, G., Coskun, A., Fouda, M. M. G. & Stoddart, J. F. Mechanically interlocked molecules assembled by π–π recognition. *ChemPlusChem.* **77**, 159–185 (2012).
18. Denis, M. & Goldup, S. M. The active template approach to interlocked molecules. *Nat. Rev. Chem.* **1**, 0061 (2017).
19. Kubota, N., Segawa, Y. & Itami, K. η^6-Cycloparaphenylene transition metal complexes: synthesis, structure, photophysical properties, and application to the selective monofunctionalization of cycloparaphenylenes. *J. Am. Chem. Soc.* **137**, 1356–1361 (2015).
20. Van Raden, J. M., Louie, S., Zakharov, L. N. & Jasti, R. 2,2′-Bipyridyl-embedded cycloparaphenylenes as a general strategy to investigate nanohoop-based coordination complexes. *J. Am. Chem. Soc.* **139**, 2936–2939 (2017).
21. Van Raden, J. M., White, B. M., Zakharov, L. N. & Jasti, R. Nanohoop rotaxanes from active metal template syntheses and their potential in sensing applications. *Angew. Chem. Int. Ed.* **58**, 7341–7345 (2019).

22. Fan, Y. Y. et al. An isolable catenane consisting of two Möbius conjugated nanohoops. *Nat. Commun.* **9**, 3037 (2018).
23. Berná, J. et al. Cadiot–Chodkiewicz active template synthesis of rotaxanes and switchable molecular shuttles with weak intercomponent interactions. *Angew. Chem. Int. Ed.* **47**, 4392–4396 (2008).
24. Movsisyan, L. D. et al. Polyyne rotaxanes: stabilization by encapsulation. *J. Am. Chem. Soc.* **138**, 1366–1376 (2016).
25. Hashimoto, S. et al. Synthesis and physical properties of polyfluorinated cycloparaphenylenes. *Org. Lett.* **20**, 5973–5976 (2018).
26. Coropceanu, V. et al. Charge transport in organic semiconductors. *Chem. Rev.* **107**, 926–952 (2007).
27. Slater, A. G. & Cooper, A. I. Function-led design of new porous materials. *Science* **348**, aaa8075 (2015).
28. Darzi, E. R. & Jasti, R. The dynamic, size-dependent properties of [5]–[12]cycloparaphenylenes. *Chem. Soc. Rev.* **44**, 6401–6410 (2015).

Methods

General protocol for active-template reactions

To a flame-dried flask equipped with stir bar were added the macrocyclic ligand (1.0 equiv.), terminal alkyne (2.5 equiv.), alkyne halide (2.5 equiv.) and $[Cu(MeCN)_4]PF_6$ (0.9 equiv.). The flask was then evacuated and backfilled with N_2 three times before introducing degassed $CHCl_3$. $[Cu(MeCN)_4]PF_6$ was slow to dissolve in $CHCl_3$, so the mixture was sonicated while sparging with N_2 until the catalyst completely dissolved. Complete dissolution of the $[Cu(MeCN)_4]PF_6$ is important to ensure that all the Cu^I ions are able to interact with the macrocyclic ligand and effectively template the cross-coupling reaction. Once the catalyst dissolved, the reaction was heated to 50 °C. Once temperature was reached, $(^iPr)_2NEt$ (2.5 equiv.) was added, which typically caused the reaction to turn from a pale yellow colour to bright orange. It was found that adding $(^iPr)_2NEt$ to the reaction mixture at 50 °C provided higher yields of the interlocked products in comparison to those of reactions in which the base was added prior to heating. Once $(^iPr)_2NEt$ was added, the reaction typically reached completion between 1.5 and 3 h. The reaction mixture was then transferred into a separatory funnel along with an aqueous solution of ammonia (18 w/w%) that contained ethylenediaminetetraacetic acid disodium salt (NH_3-EDTA). The mixture was emulsified and allowed to separate twice before the organic layer was collected. The aqueous layer was extracted with an additional portion of fresh dichloromethane (DCM) and the organic layers were combined and dried over Na_2SO_4. The reaction products were separated via column chromatography (**6a**, **6b**, **6g** and **6i**: SiO_2, 0–15% DCM in hexanes to elute the freely cross-coupled threads; 15–40% DCM in hexanes to elute the mechanically interlocked product; 0–5% EtOAc in hexanes to elute 'unreacted' macrocyclic ligand); (**6e**: SiO_2, 0–15% DCM in hexanes to elute the freely cross-coupled threads; 15–100% DCM in hexanes to elute the mechanically interlocked product; 0–10% EtOAc in hexanes to elute 'unreacted' macrocyclic ligand).

Data availability

Experimental procedures for the synthesis of all the compounds are available in the Supplementary Information. Crystallographic data for the structures reported in this article have been deposited at the Cambridge Crystallographic Data Centre, under deposition numbers CCDC 2159304 (**1a**), 2159303 (**1b**), 2159302 (**2**), 2159305 (diaza[8]CPP) and 2159306 (diaza[9]CPP). Copies of the data can be obtained free of charge via https://www.ccdc.cam.ac.uk/structures/. In addition to the spectra provided in the Supplementary Information, raw ^1H and ^{13}C data for all the novel structures are provided as Supplementary Data 6.

Acknowledgements

This project was supported by the National Science Foundation (CHE-1808791). J.H.M. and R.L.M. were additionally supported by National Science Foundation Graduate Research Fellowships.

Author contributions

J.H.M., J.M.V.R. and R.J. were responsible for the conceptualization of the project. All the synthetic steps reported were performed by J.H.M. along with the computational and photophysical analyses. J.H.M. and R.J. drafted the original version of the manuscript with editing from J.M.V.R. and R.L.M. L.N.Z. collected and analysed all the crystallographic data.

Competing interests

The authors declare no competing interests.

Additional information

Supplementary information The online version contains supplementary material available at https://doi.org/10.1038/s41557-022-01106-9.

Correspondence and requests for materials should be addressed to Ramesh Jasti.

Peer review information *Nature Chemistry* thanks Birgit Esser and the other, anonymous, reviewer(s) for their contribution to the peer review of this work.